Identifying Shared Neuroanatomic Architecture Between Cognitive Traits Through Multiscale Morphometric Correlation Analysis

Zixuan Wen[1], Jingxuan Bao[1], Shu Yang[1], Shannon L. Risacher[2], Andrew J. Saykin[2], Paul M. Thompson[3], Christos Davatzikos[1], Heng Huang[4], Yize Zhao[5], and Li Shen[1(✉)]

[1] University of Pennsylvania, Philadelphia, PA, USA
li.shen@pennmedicine.upenn.edu
[2] Indiana University, Indianapolis, IN, USA
[3] University of Southern California, Los Angels, CA, USA
[4] University of Maryland, College Park, MD, USA
[5] Yale University, New Haven, CT, USA

Abstract. We introduce an informative metric, called morphometric correlation, as a measure of shared neuroanatomic similarity between two cognitive traits. Traditional estimates of trait correlations can be confounded by factors beyond brain morphology. To exclude these confounding factors, we adopt a Gaussian kernel to measure the morphological similarity between individuals and compare pure neuroanatomic correlations among cognitive traits. In our empirical study, we employ a multiscale strategy. Given a set of cognitive traits, we first perform morphometric correlation analysis for each pair of traits to reveal their shared neuroanatomic correlation at the whole brain (or global) level. After that, we extend our whole brain concept to regional morphometric correlation and estimate shared neuroanatomic similarity between two cognitive traits at the regional (or local) level. Our results demonstrate that morphometric correlation can provide insights into shared neuroanatomic architecture between cognitive traits. Furthermore, we also estimate the morphometricity of each cognitive trait at both global and local levels, which can be used to better understand how neuroanatomic changes influence individuals' cognitive status.

Keywords: Brain image analysis · Morphometricity · Morphometric Correlation · Cognitive Traits · Alzheimer's Disease

Z. Wen and J. Bao—These authors contributed equally to this work.

This work was supported in part by the NIH grants U01 AG068057, RF1 AG063481, U01 AG066833, R01 LM013463, P30 AG073105, and R01 AG071470, and the NSF grant IIS 1837964. Data used in this study were obtained from the Alzheimer's Disease Neuroimaging Initiative database (adni.loni.usc.edu), which was funded by NIH U01 AG024904.

J. Woo et al. (Eds.): MICCAI 2023 Workshops, LNCS 14394, pp. 227–240, 2023.
https://doi.org/10.1007/978-3-031-47425-5_21

1 Introduction

To date, magnetic resonance imaging (MRI) scans have been widely used in many anatomical studies of the human brain [12,13,15]. In brain disorder studies, it is an important research topic to identify pathological changes in the brain. Most neurodegenerative diseases, such as Alzheimer's Disease (AD), together with cognitive impairments can be detected through brain atrophy patterns captured by structural MRI (sMRI). Several automated techniques have been developed to assess brain atrophy. Voxel-based morphometry (VBM) [1,20] is one of the widely used techniques that provide biologically plausible results by voxel-wise statistical tests to identify brain anatomy differences between different populations.

Recently, substantial attention has been given to mapping associations between neuroanatomic features and complex behavioral or cognitive traits in the field of brain image analysis [15–17,21]. The concept of "morphometricity" [11] was first proposed to measure the proportion of a trait variance explained by neuroanatomic features in the brain. Grey-matter correlation [3] was introduced to capture the shared morphometricity of two quantitative traits. Both in the morphometricity [11] study and the grey-matter correlation [3] study, the whole brain morphology measurements were used and detailed ROI-level signatures were ignored. Thus, in this work, we propose an informative metric, named "morphometric correlation" and construct the morphological similarity matrix using the Gaussian kernel to measure and reveal the shared neuroanatomic signatures across cognitive traits. Furthermore, we employ a multiscale strategy and extend the concept of morphometricity and morphometric correlation from its original definitions at the whole brain (or global) level to a more focal (or local) level based on a region of interest (ROI).

Our contributions can be summarized as follows.

1. Traditional estimates of correlations between two cognitive traits are confounded by factors beyond the brain morphology. We introduce morphometric correlation, as a measure of shared neuroanatomic similarity between two cognitive traits.
2. We propose a non-linear (Gaussian) kernel to construct the similarity relationship matrix. The Gaussian kernel can better capture nonlinear and multivariate associations between genes and traits [9]. We demonstrate in our empirical study that the proposed Gaussian kernel can capture more neuroanatomic signatures than the traditional linear kernel used in grey-matter correlation [3].
3. The previous studies [2,3,11] only applied region of interest (ROI) analysis on the study of morphometricity. In this work, we perform a multiscale morphometric correlation analysis. Specifically, we extend the whole brain morphometric correlation to the local level and estimate shared neuroanatomic similarity between two cognitive traits at the regional (or local) level.
4. Our empirical study has yielded multiple interesting findings. We have observed that the estimated morphometric correlations are stronger than the

direct phenotypic correlations between most cognitive trait pairs, except for the morphometric correlation between MMSE and ADAS13. The ROI-based morphometric correlation between MMSE and ADAS13 using our multiscale strategy can identify multiple ROIs that capture more shared morphological signatures than the whole brain. At the same time, we also compute the whole brain and ROI-based morphometricity. It suggests cognitive traits MMSE and ADAS13 are most associated with the human brain.

Our study can quantify statistical associations between neuroanatomic features and cognitive phenotypes at the population level. The algorithm we use is computationally efficient in the way that it estimates the (co)variance parameters without cross-validation. Our study provides new insights to investigate the associations between the cognition and brain morphology. Whole brain morphometricity and morphometric correlation are biologically interpretable, and could be used to conduct morphological and cognitive studies in the future. Furthermore, our proposed multiscale strategy can better discover the ROI-level imaging cognition associations and reveal the correlation between two cognitive measurements captured by ROI-level brain morphology.

2 Methods

We summarize our overall experimental pipeline in Fig. 1. The pipeline is designed to identify brain imaging cognition associations at multiple scales: one revealed by the whole brain (global) measurements and the other revealed by the ROI-based (local) measurements. First, we use Statistical Parametric Mapping [1,20] to automatically process sMRI scans and obtain the volumetric summary statistics of each voxel. Voxel-based morphometry (VBM) constitutes a comprehensive measurement of the structural anatomy. Next, we use Gaussian kernel [9] to calculate the pairwise morphological similarity between individuals and obtain a morphological relationship matrix (MRM). First of all, we construct the MRM using all the voxels within the whole brain. After that, we construct the MRM using all the multivariate voxel measures within each ROI. Finally, based on global MRM (or local MRM), we estimate whole brain (or ROI-based) morphometricity and morphometric correlation using the average information restricted maximum likelihood (REML) algorithm. Our simulation experiment demonstrates that applying the Gaussian kernel can be less confounded by factors beyond brain morphology. In the real data experiment, 185,405 voxels are used to analyze the whole-brain morphometricity and morphometric correlation across seven clinical cognitive assessment scores in ADNI [18,19] dataset. Then, we extend our method to explore morphometric patterns at the ROI level instead of the global neuroanatomy by estimating the ROI-based morphometricties and morphometric correlations. Our results demonstrate the promise of our proposed method in offering a unique perspective to reveal the underlying neuroanatomic relationship among cognitive traits.

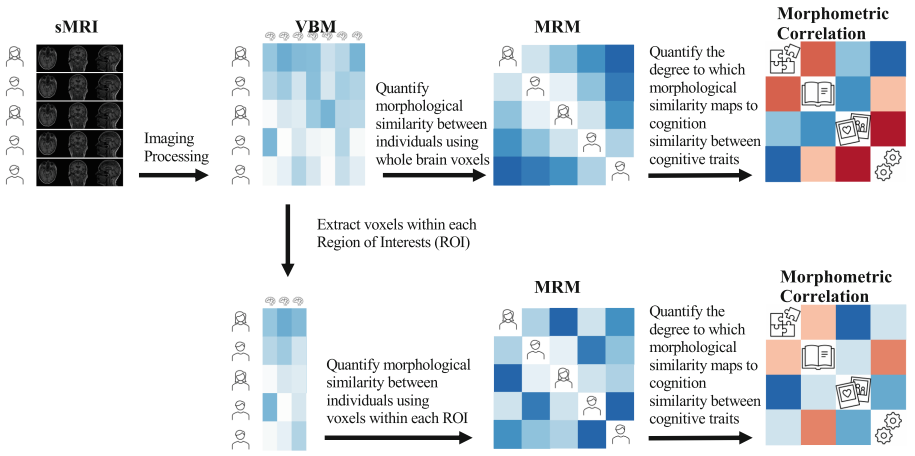

Fig. 1. Morphometric Correlation Analysis Pipeline. Structural MRI scans are processed to obtain voxel-based morphometry (VBM). We first construct a morphological relationship matrix (MRM) using voxels within whole brain. Then, we use this MRM to obtain global morphometricity and morphometric correlation via average information REML algorithm. After that, we construct several morphological relationship matrices using voxels within each ROI. Then, we obtain ROI-based morphometricity and morphometric correlation based on these MRMs

2.1 Bivariate Linear Mixed Effect Model

The morphometricity and morphometric correlation are grounded in the following bivariate linear mixed effect (LME) model [7]:

$$\begin{aligned} y_1 = &\quad Xb_1 + a_1 + \varepsilon_1, \\ y_2 = &\quad Xb_2 + a_2 + \varepsilon_2, \end{aligned} \tag{1}$$

where y_i is an $n \times 1$ vector of a quantitative phenotype trait i with n being the number of subjects, b_i is a $s \times 1$ vector of fixed effect, X is an $n \times s$ matrix of confounding variables with s being the number of confounding variables, a_i is an $n \times 1$ vector of random effects with $a_i \sim N(0, A\sigma^2_{a_i})$ and $\varepsilon_i \sim N(0, I\sigma^2_{\varepsilon_i})$ is the error term. A is interpreted as the morphological relationship matrix (MRM). MRM quantifies the morphological similarity between two individuals using brain morphology measurements. We use the Gaussian-type similarity metric to accurately measure the similarity from sMRI scan morphometry. The (k, j)-th entry of MRM [9,11] is defined as

$$A_{kj} = \exp\left(-\sum_l \frac{(z_{kl} - z_{jl})^2}{ms_l^2}\right), \tag{2}$$

where z_{kl} is the (k,l)-th elements of imaging measurements matrix Z, refers to the morphometry of l-th voxel of k-th subjects, s_l is the sample standard error of the l-th voxel and m is the number of voxels.

The difference between the morphological relationship matrix and brain relatedness matrix (BRM) used in grey-matter correlation [3] is the method to construct the relationship matrix. Brain relatedness matrix B use linear kernel to quantify the similarities between individuals, which is defined as $B = \frac{1}{m}\widetilde{Z}\widetilde{Z}^T$, where m is the number of measurements, in this case, m is the number of voxels and $\widetilde{Z}$ is a standardized brain imaging measurement matrix.

Formally, the morphometricity of a given trait [11] is the proportion of its phenotypic variation that can be explained by brain morphology, the variation of which is captured by MRM. The morphometricity for trait i can be defined as

$$m_i^2 = \frac{\sigma_{a_i}^2}{\sigma_{a_i}^2 + \sigma_{\varepsilon_i}^2}, \tag{3}$$

where $\sigma_{a_i}^2$ is the phenotypic variance explained by brain morphology, and $\sigma_{a_i}^2 + \sigma_{\varepsilon_i}^2$ is the total phenotypic variance.

Morphometric correlation then measures the degree of brain morphology similarity to which two traits have in common, the correlation of which is captured by MRM. We define the morphometric correlation as

$$r^2 = \frac{\rho}{\sqrt{\sigma_{a_1}^2 \sigma_{a_2}^2}}, \tag{4}$$

where ρ is the covariance between the brain voxels associations with each trait.

We can therefore obtain morphometricity and morphometric correlation by estimating variance and covariance parameters $\theta = (\sigma_{a_1}^2, \sigma_{\varepsilon_1}^2, \sigma_{a_2}^2, \sigma_{\varepsilon_2}^2, \rho)$. The estimators are usually obtained by maximizing a log-likelihood function.

2.2 Efficient Average Information REML Algorithm

The average information restricted maximum likelihood (REML) algorithm has been widely used in estimating variance and covariance parameters [3,8,22]. The average information matrix has been proved [8,23] much more computationally efficient than the observed information matrix [5,10] and Fisher information matrix [5,6]. By assuming bivariate normality of two traits y_1, y_2, the joint distribution of two traits can be written as

$$y = \begin{bmatrix} y_1 \\ y_2 \end{bmatrix} \sim N\left(\begin{bmatrix} X & 0 \\ 0 & X \end{bmatrix} \begin{bmatrix} b_1 \\ b_2 \end{bmatrix}, \mathbf{V}(\theta) \right), \tag{5}$$

The variance matrix $\mathbf{V}(\theta)$ is defined as

$$\mathbf{V}(\theta) = \begin{bmatrix} A\sigma_{a_1}^2 + I\sigma_{\varepsilon_1}^2 & A\rho \\ A\rho & A\sigma_{a_2}^2 + I\sigma_{\varepsilon_2}^2 \end{bmatrix}, \tag{6}$$

where A is the morphological relationship matrix defined in Eq. (2), and I is an $n \times n$ identity matrix. $\sigma^2_{a_i}$ and $\sigma^2_{\varepsilon_i}$ are morphometric variance and residual variance of trait i, respectively, and ρ is the morphometric covariance.

We obtain the estimators by maximizing the restricted log-likelihood function of Eq. (5) (ignoring the constant), $l = -\frac{1}{2}\big(\log|\mathbf{V}(\theta)| + \log|X^T\mathbf{V}(\theta)^{-1}X| + y^TPy\big)$, where $|\cdot|$ refers to the determinant of the matrices. And the matrix P is defined as

$$P = \mathbf{V}(\theta)^{-1} - \mathbf{V}(\theta)^{-1}X(X^T\mathbf{V}(\theta)^{-1}X)^{-1}X^T\mathbf{V}(\theta)^{-1}. \tag{7}$$

We use restricted maximum likelihood (REML) rather than maximum likelihood (ML) due to the unbiasedness of REML estimation of (co)variance parameters $\widehat{\theta}_{\mathrm{REML}} = \mathrm{argmax}_\theta\, l$.

Next, the score function $S(\theta)$ is defined as $S(\theta_i) = \frac{\partial l}{\partial \theta_i} = -\frac{\mathrm{tr}(P\dot{V}_i) - y^TP\dot{V}_iPy}{2}$, where $\mathrm{tr}(\cdot)$ is the trace of the matrix and the (i,j)-th entry of average information matrix [4] is defined as

$$\mathbf{AI}(\theta)_{ij} = \frac{y^TP\dot{V}_iP\dot{V}_jPy}{2}, \tag{8}$$

where $\dot{V}_i = \frac{\partial \mathbf{V}(\theta)}{\partial \theta_i}$.

The initial guess of parameters is given by arbitrary values. In the first step, we update the parameters using the expected maximization (EM) algorithm, $\theta_i^{(1)} \leftarrow \theta_i^{(0)} + \frac{1}{n}\theta_i^{2(0)}S(\theta_i^{(0)})$. Then, our method switches to the average information REML algorithm, $\theta^{(t+1)} \leftarrow \theta^{(t)} + \mathbf{AI}(\theta^{(t)})^{-1}S(\theta^{(t)})$, updating parameters until the log-likelihood function satisfies the criteria $l^{(t+1)} - l^{(t)} \leq 10^{-4}$. In the iteration process, if any parameters $\sigma^2_{a_i}$ or $\sigma^2_{\varepsilon_i}$ escape from the parameter space, i.e. if $\sigma^2_{a_i}$ or $\sigma^2_{\varepsilon_i}$ is less than 0, it will be set to $10^{-6} \times \sigma^2_{y_i}$. For parameter ρ, if its absolute value $|\rho|$ larger than $\sqrt{\sigma^2_{a_1}\sigma^2_{a_2}}$, it will be set to $\rho = \mathrm{sign}(\mathrm{Cov}\,(y_1, y_2))\sqrt{\sigma^2_{a_1}\sigma^2_{a_2}}$, where $\mathrm{sign}(\cdot)$ is the signum function.

Significance testing of morphometricity estimates m_i^2 can be obtained via the likelihood ratio test (LRT). Under the null hypothesis ($\sigma^2_{a_i} = 0$), the LRT statistic follows $\frac{1}{2}\chi^2_0 + \frac{1}{2}\chi^2_1$, where χ^2_1 is one degree of freedom χ^2 distribution and χ^2_0 is χ^2 distribution with all probability mass at zero. Similarly, the significance testing for correlation coefficient ρ can also be obtained via LRT.

3 Experimental Results

3.1 Materials

The neuroimaging, demographic, and clinical cognitive assessment data used in the preparation of this article were obtained from the Alzheimer's Disease Neuroimaging Initiative (ADNI) database (http://adni.loni.usc.edu) [18,19]. The ADNI was launched in 2003 as a public-private partnership, led by Principal Investigator Michael W. Weiner, MD. The primary goal of ADNI has been to test

whether serial magnetic resonance imaging (MRI), positron emission tomography (PET), other biological markers, and clinical and neuropsychological assessment can be combined to measure the progression of mild cognitive impairment (MCI) and early Alzheimer's disease (AD). Up-to-date information about the ADNI is available at www.adni-info.org.

Structural MRI scans were processed with voxel-based morphometry (VBM) using the Statistical Parametric Mapping (SPM) software tool [1]. All scans were aligned to a T1-weighted template image, segmented into gray matter (GM), white matter (WM), and cerebrospinal fluid (CSF) maps, normalized to the standard Montreal Neurological Institute (MNI) space as $2 \times 2 \times 2$ mm^3 voxels. The GM maps were extracted and smoothed with an 8 mm FWHM kernel, and analyzed in this study. A total of 185,405 non-background voxels, covering cortical, sub-cortical, and cerebellar regions and measuring GM density, were studied in this work as whole brain morphology measurements. Based on the AAL atlas [14], 116 ROI-based morphology measurements are constructed by selecting the voxel-level measurements within each ROI.

Age and gender were used as covariates, following a prior study [11]. Our analysis included seven clinical cognitive assessment scores from the QT-PAD project (http://www.pi4cs.org/qt-pad-challenge). These cognitive scores are Alzheimer's Disease Assessment Scale (ADAS13), Clinical Dementia Rating Sum of Boxes (CDRSB), Rey Auditory Verbal Learning Test (RAVLT.learning), Rey Auditory Verbal Immediate Test (RAVLT.immediate), Rey Auditory Verbal Forgetting Test (RAVLT.forgetting), Mini-Mental State Exam (MMSE), and Functional Activities Questionnaire (FAQ). All subjects with no missing cognitive measures and sMRI measures of the first visit were included in this study. After data preprocessing, there are 1,451 participants ($n = 1,451$) left, including 821 males and 630 females. The average age of participants is 73.9, and the standard deviation of age is 7.1.

3.2 Simulation Results

To show the superior performance of the Gaussian kernel, we also implement the linear kernel for comparison on the simulated data. We first generate 100 pairs of synthetic quantitative traits with joint distribution as shown in Eq. (5). The brain morphometry matrix Z used in the simulation experiment is the left hippocampus voxel-based morphometry. Then the Gaussian kernel MRM A can be obtained by Eq. (2), and the linear kernel BRM B can be obtained by doing the inner product of normalized Z and Z^T. To meet the normality assumption of the model, we first uniformly simulate $\sigma^2_{a_i}$ from $[0, 1]$, then let $\sigma^2_{\varepsilon_i} = 1 - \sigma^2_{a_i}$, we also uniformly simulate ρ from $[0, 1]$. Then we could obtain ground truth morphometricity and morphometric correlation based on Eq. (3) and Eq. (4) respectively. Next, pair (a_1, a_2) is simulated from bivariate normal distribution

$$\begin{bmatrix} a_1 \\ a_2 \end{bmatrix} \sim N\left(\begin{bmatrix} 0 \\ 0 \end{bmatrix}, \begin{bmatrix} \sigma^2_{a_1} A & \rho A \\ \rho A & \sigma^2_{a_2} A \end{bmatrix} \right),$$

ε_i is simulated from normal distribution $N(0, (1-\sigma^2_{a_i})I_{n\times n})$, where $I_{n\times n}$ is the n by n identity matrix. The confounding variables we select are age and gender variables. Finally, we have the two traits y_1 and y_2 by Eq. (1). We then estimate the variance and covariance parameters of synthetic quantitative traits using the average information REML algorithm. Once we obtain the estimated $\sigma^2_{a_i}$, $\sigma^2_{\varepsilon_i}$ and ρ, the estimated morphometricity and morphometric correlation can be obtained by Eq. (3) and Eq. (4) respectively.

Figure 2**A** and Fig. 2**B** show the comparisons between estimated morphometricities using MRM and BRM [3] respectively. The estimated morphometricity using our method shows better concordance with the synthetic morphometricity, in which the correlation between synthetic and estimated morphometricty is 0.99 (Fig. 2**A**). The correlation between synthetic and estimated morphometricty using the linear kernel is 0.96 (Fig. 2**B**), which indicates linear kernel is also reliable in practice. The simulation comparison of morphometricity estimations suggests our method is more accurate than the linear kernel method.

Comparisons of estimated morphometric correlations using different relationship matrices are shown in Fig. 2**C** (MRM) and Fig. 2**D** (BRM) [3] respectively. Most of the Gaussian-based estimated morphometric correlations are concordance with the synthetic morphometric correlations (the correlation is 0.95 in Fig. 2**C**). It indicates that the estimated morphometric correlation is approximately the same as the truth morphometric correlation. However, Fig. 2**D** reveals the correlation between ground truth and estimated morphometric correlation is only 0.89, which is less accurate. These two figures show that the Gaussian kernel is more reliable and accurate in the morphometric correlation analysis. Estimated morphometric correlation also suggests that morphometric correlation between two traits is not reliable when the morphometricity of either trait is small.

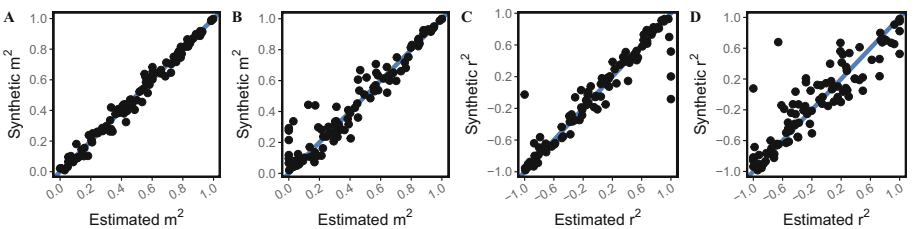

Fig. 2. Comparison of true and estimated morphometricities using different similarity matrix **A.** MRM and **B.** BRM. Comparison of true and estimated morphometric correlation using different similarity matrix **C.** MRM and **D.** BRM.

3.3 Whole Brain Morphometric Correlation and Morphometricity

The traditional phenotypic correlation can be confounded by factors beyond brain morphology. Simulation results indicate that MRM is much more accu-

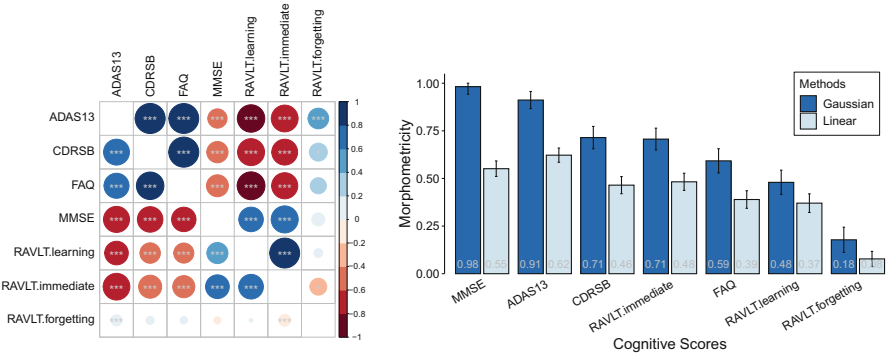

(a) Morphometric Correlation (b) Morphometricity

Fig. 3. (a) Morphometric correlation among seven cognitive traits. Upper triangle shows the morphometric correlation between two traits, while lower triangle is the phenotypic correlation between pairs of traits. An asterisk indicates significance with $p < 0.05$, two asterisks indicate significance with $p < 0.01$, three asterisks indicates significance with $p < 0.001$. (b) Morphometricity estimations of seven cognitive traits using Gaussian and linear kernel. Error bars indicate SE of the estimates.

rate than BRM when estimating the morphometric correlation. Besides, the grey-matter correlation strategy [3] failed to estimate the brain morphometric correlation between two given cognitive traits in our real experiment. Thus, we present our estimated pairwise morphometric correlations in Fig. 3(a), which reveal the shared neuroanatomic similarity between two cognitive traits. The lower triangle shows the phenotypic correlation between two traits, which is the Pearson correlation between two traits. The upper triangle is our estimated morphometric correlation. The morphometric correlation and phenotypic correlation among seven cognitive traits have the same direction, except for the correlation between MMSE and RAVLT.forgetting. Most of the morphometric correlation and phenotypic correlation are significant ($p < 0.005$). The largest positive morphometric correlation is $\widehat{r}^2 = 0.98$, which is presented between ADAS13 and CDRSB, as well as between FAQ and CDRSB. Besides, both the morphometric correlation between ADAS13 and FAQ and the morphometric correlation between RAVLT.learning and RAVLT.immediate are large (with $\widehat{r}^2 = 0.97$). They are larger than their underlying phenotypic correlation. The largest negative correlation is founded between FAQ and RAVLT.learning ($\widehat{r}^2 = -0.85$), whose corresponding phenotypic correlation is only -0.44.

The morphometric correlation between ADAS13 and MMSE (-0.4) is not as strong as their phenotypic correlation (-0.74). First note that, the negative correlation is reasonable, since the lower scores of MMSE indicating of poorer performance and greater cognitive impairment, while higher scores of ADAS13 reflect poorer performance. Next, this result indicates that the shared brain morphology variants of two traits are able to weaker than their shared phenotypic variants. Finally, we notice that the detailed regional associations can be ignored

when using whole brain morphology. This evidence motivates our ROI-based morphometric correlation study.

Simulation results indicate the Gaussian kernel is slightly more accurate than the linear kernel. The results of whole brain morphometricity estimations again demonstrate that the Gaussian kernel can capture more neuroanatomic signatures than the linear kernel. We compare brain morphometricity of seven cognitive traits using Gaussian kernel or linear kernel in Fig. 3(b). These cognitive traits are widely used in measuring cognition impairment and memory loss. The morphometricity results estimated by the Gaussian kernel are much higher than that used by the linear kernel, especially for traits MMSE and ADAS13. All the cognitive traits are statistically significantly associated with whole brain morphology (all the p-value are less than 0.005). The Gaussian-based MRM results reveal that MMSE and ADAS13 are substantially morphometric (with point estimates of 0.98 and 0.91 respectively), suggesting that these two cognitive traits are associated with substantial anatomical signatures. However, morphometricity values of CDRSB, RAVLT.immediate, FAQ, and RAVLT.learning are moderate, all greater than 0.4. Finally, the estimated morphometricity value of RAVLT.forgetting is only 0.18, which indicates only 18% of variation of RAVLT.forgetting traits could be explained by brain morphometry.

In practice, the MMSE score is frequently used for Alzheimer's disease drug studies and the ADAS13 score evaluates memory, reasoning, and language. Our method also reveals that these two traits are associated with substantial anatomical signatures.

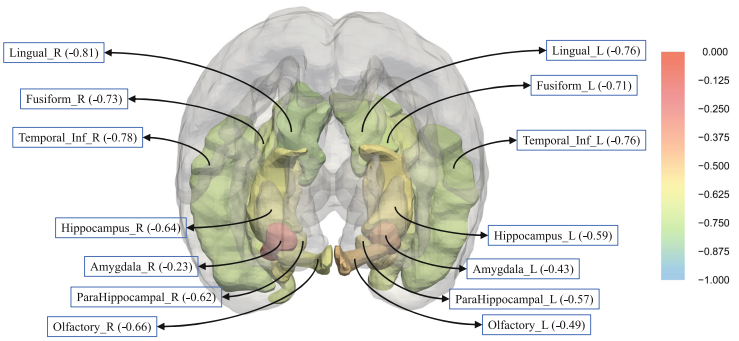

Fig. 4. ROI-based morphometric correlation between ADAS13 and MMSE. The ROIs are those most related to AD.

3.4 Brain ROI-Based Morphometric Correlation and Morphometricity

To reveal ignored morphometric correlations at the regional level, we apply the multiscale strategy by using the voxels within each ROI instead of the whole

brain as morphology measurements. Then, we calculate the local (regional) MRM and the variation that could be captured by the local MRM. The extension is important since the spatial association between brain morphology and cognitive traits can not be revealed when using whole brain morphometry. We choose and analyze 14 regions that are most related to AD and reveal the ROI-based morphometric correlation between MMSE and ADAS13. Figure 4 shows the spatial map and values of ROI level morphometric correlation between MMSE and ADAS13. The ROI level morphometric correlation can be larger than that using whole brain morphometry. The shared morphological architectures captured by all AD related regions (except region `Amygdala_R`) are larger than that captured by the whole brain (−0.40). Especially, regions `Lingual_R`, `Temporal_Inf_R`, `Temporal_Inf_L`, and `Lingual_L` show the morphometric correlation between two traits are even larger than their phenotypic correlation (−0.74). This finding suggests that some regions are stronger to capture the association between two cognitive traits than the whole brain. Figure 4 also indicates most regions in the right brain can capture more similarity of two traits than regions in the left brain. This evidence is promising and has an important impact on revealing structure changes within ROIs from an evolutionary morphological perspective.

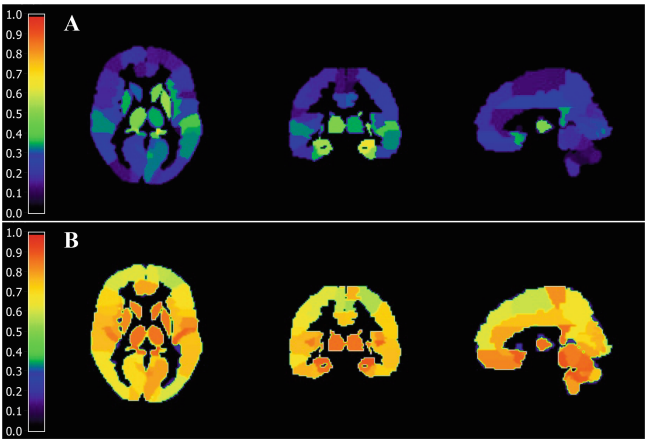

Fig. 5. ROI-based morphometricity of **A.** ADAS13 and **B.** MMSE.

We have shown in Fig. 3(b), MMSE and ADAS13 have substantial neuroanatomic signatures associated with brain morphology. Then, we extend our analysis to the ROI-level morphometricity of ADAS13 and MMSE using multiscale strategy. At this time, we estimate associations between 116 regions and cognitive traits. The regional level morphometricity of these two cognitive traits is shown as spatial morphometricity heatmap in Fig. 5. In contrast to the whole brain morphometricity of ADAS13 cognitive trait (0.91), the top 5 ROIs which are identified as having substantial association with the ADAS13 are `Pallidum_R` (0.67), `Hippocampus_L` (0.66), `Amygdala_L` (0.65),

ParaHippocampal_L (0.61), Hippocampus_R (0.55). For MMSE, the top 5 ROIs are Vermis_1_2 (0.93), Pallidum_R (0.93), Vermis_10 (0.91), Hippocampus_R (0.91), Amygdala_L (0.90). Both ADAS13 and MMSE are highly associated with regions Hippocampus and Amygdala, which suggests our multiscale strategy can provide strong evidence in prioritizing regions that are more related to the given phenotype. Thus, our regional morphometricity strategy bridges the gap that regional information is ignored by whole brain morphometricity.

The spatial morphometricity map also reveals the nonsymmetric distributed morphometricity, suggesting that the variation of cognitive scores captured by ROIs are not equal for left and right regions. The ROI level morphometricity analysis is able to identify relevant neuroimaging biomarkers and to explain brain structure variants related to cognitive variants.

4 Conclusion and Discussions

In this study, we have introduced a novel concept "morphometric correlation" as a measure of the morphological signatures shared by complex traits. To exclude the effect caused by factors other than brain morphology, we have adopted a Gaussian kernel to construct the relationship matrix and average information REML algorithm to obtain unbiased estimates of the morphometric correlation. The estimated morphometric correlation is able to quantify the neuroanatomic aggregate features of pairs of quantitative traits. The superiority of our method has been demonstrated by both simulation results and the applications of estimating morphometric correlations among cognitive traits. We then use a multiscale strategy to extend the concept to the local level by using the voxels within each ROI.

We have observed that the estimated morphometric correlations are stronger than the pure phenotypic correlations between most pairs of cognitive traits. Both the morphometric correlation of ADAS13 and CDRSB and the morphometric correlation of CDRSB and FAQ are significantly high ($\widehat{r}^2 = 0.97, p < 0.001$). The morphometric correlation of FAQ and RAVLT.learning is significantly low ($\widehat{r}^2 = -0.85, p < 0.001$). Although the whole brain morphometric correlation between MMSE and ADAS13 is not as strong as the corresponding phenotypic correlations, the ROI-based morphometric correlation identifies some ROIs that capture more shared morphological signatures than the whole brain. The prioritized ROIs may provide new insights for future brain morphology and cognition studies.

We have also estimated the morphometricity of cognitive traits, which is the proportion of the phenotypic variation captured by the brain morphology. In the application to the whole brain morphometricity analysis, our method was able to accurately reveal the variation explained by brain morphology. The cognitive traits MMSE and ADAS13 are substantially morphometric. However, the ROI-based morphometricity of MMSE is moderate, while the ROI-based morphometricity of ADAS13 is modest. The ROI level morphometricity analysis provides important information for understanding brain structural variation related to cognitive variation and can potentially help characterize the progression of AD.

References

1. Ashburner, J., Friston, K.J.: Voxel-based morphometry-the methods. Neuroimage **11**(6), 805–821 (2000)
2. Bao, J., et al.: Identifying imaging genetic associations via regional morphometricity estimation. In: Pacific Symposium on Biocomputing, vol. 27, pp. 97–108 (2022)
3. Couvy-Duchesne, B., et al.: A unified framework for association and prediction from vertex-wise grey-matter structure. Hum. Brain Mapp. **41**(14), 4062–4076 (2020)
4. Gilmour, A.R., Thompson, R., Cullis, B.R.: Average information REML: an efficient algorithm for variance parameter estimation in linear mixed models. Biometrics 1440–1450 (1995)
5. Harville, D.A.: Maximum likelihood approaches to variance component estimation and to related problems. J. Am. Stat. Assoc. **72**(358), 320–338 (1977)
6. Jennrich, R.I., Sampson, P.: Newton-raphson and related algorithms for maximum likelihood variance component estimation. Technometrics **18**(1), 11–17 (1976)
7. Laird, N.M., Ware, J.H.: Random-effects models for longitudinal data. Biometrics 963–974 (1982)
8. Lee, S.H., Van Der Werf, J.H.: An efficient variance component approach implementing an average information REML suitable for combined LD and linkage mapping with a general complex pedigree. Genet. Sel. Evol. **38**(1), 1–19 (2006)
9. Liu, D., Lin, X., Ghosh, D.: Semiparametric regression of multidimensional genetic pathway data: least-squares kernel machines and linear mixed models. Biometrics **63**(4), 1079–1088 (2007)
10. Meyer, K., Smith, S.: Restricted maximum likelihood estimation for animal models using derivatives of the likelihood. Genet. Sel. Evol. **28**(1), 23–49 (1996)
11. Sabuncu, M.R., Ge, T., Holmes, A.J., et al.: Morphometricity as a measure of the neuroanatomical signature of a trait. Proc. Natl. Acad. Sci. **113**(39), E5749–E5756 (2016)
12. Shen, L., et al.: ADNI: identifying neuroimaging and proteomic biomarkers for MCI and AD via the elastic net. Multimodal Brain Image Anal. **7012**, 27–34 (2011)
13. Shen, L., Thompson, P.M.: Brain imaging genomics: integrated analysis and machine learning. Proc. IEEE **108**(1), 125–162 (2020)
14. Tzourio-Mazoyer, N., et al.: Automated anatomical labeling of activations in SPM using a macroscopic anatomical parcellation of the MNI MRI single-subject brain. Neuroimage **15**(1), 273–289 (2002)
15. Wan, J., et al.: Identifying the neuroanatomical basis of cognitive impairment in Alzheimer's disease by correlation- and nonlinearity-aware sparse Bayesian learning. IEEE Trans. Med. Imaging **33**(7), 1475–1487 (2014)
16. Wang, H., Nie, F., Huang, H., Risacher, S., Saykin, A.J., Shen, L.: Identifying ad-sensitive and cognition-relevant imaging biomarkers via joint classification and regression. Med. Image Comput. Comput. Assist. Interv. **14**(Pt 3), 115–23 (2011)
17. Wang, X., et al.: Exploring automated machine learning for cognitive outcome prediction from multimodal brain imaging using streamline. AMIA Jt. Summits Transl. Sci. Proc. **2023**, 544–553 (2023)
18. Weiner, M.W., Veitch, D.P., Aisen, P.S., et al.: The Alzheimer's disease neuroimaging initiative: a review of papers published since its inception. Alzheimers Dement. **9**(5), e111-94 (2013)

19. Weiner, M.W., Veitch, D.P., Aisen, P.S., et al.: Recent publications from the Alzheimer's disease neuroimaging initiative: reviewing progress toward improved AD clinical trials. Alzheimer's Dementia **13**(4), e1–e85 (2017)
20. Wright, I., et al.: A voxel-based method for the statistical analysis of gray and white matter density applied to schizophrenia. Neuroimage **2**(4), 244–252 (1995)
21. Yan, J., et al.: Alzheimer's disease neuroimaging initiative: cortical surface biomarkers for predicting cognitive outcomes using group L2,1 norm. Neurobiol. Aging **36**(Suppl. 1), S185–S193 (2015)
22. Yang, J., Lee, S.H., Goddard, M.E., Visscher, P.M.: GCTA: a tool for genome-wide complex trait analysis. Am. J. Hum. Genet. **88**(1), 76–82 (2011)
23. Zhu, S., Wathen, A.J.: Essential formulae for restricted maximum likelihood and its derivatives associated with the linear mixed models. arXiv preprint arXiv:1805.05188 (2018)